

## THE INTERACTION WITH THE LOWER IONOSPHERE OF ELECTROMAGNETIC PULSES FROM LIGHTNING: EXCITATION OF OPTICAL EMISSIONS

Y.N. Taranenko, U.S. Inan, and T.F. Bell

STAR Laboratory, Stanford University

**Abstract.** A self consistent and fully kinetic simulation of the interaction of lightning radiated electromagnetic (EM) pulses with the nighttime lower ionosphere indicates that optical emissions observable with conventional instruments would be excited. For example, emissions of the 1st and 2nd positive bands of  $N_2$  occur at rates reaching  $7 \times 10^7$  and  $10^7 \text{ cm}^{-3} \text{ s}^{-1}$  respectively at  $\sim 92 \text{ km}$  altitude for a lightning discharge with an electric field  $E_{100} = 20 \text{ V/m}$  (normalized to a 100 km distance). The maximum height integrated intensities of these emissions are  $4 \times 10^7$  and  $6 \times 10^6 \text{ R}$  respectively, lasting for  $\sim 50 \mu\text{s}$ .

## 1. Introduction

In a recent paper [Taranenko et al., 1993, hereafter referred to as I] we used a kinetic formulation of the electron dynamics and Maxwell's equations for the EM fields to self consistently simulate the interaction of lightning radiated EM pulses with the lower ionosphere. We found that under nighttime conditions, individual pulses of intensity  $E_{100} \sim 10\text{-}20 \text{ V/m}$  produce changes in electron density in the range of 1 to 30% of the ambient due to ionization and dissociative attachment induced by the heated electrons. In this paper, we apply the same technique to calculate the excitation of optical emissions, which is a natural consequence of such heating. A first estimate of the optical emission spectra was provided in an earlier model which assumed a Maxwellian distribution and neglected reflection of the wave from the ionosphere [Taranenko et al., 1992].

## 2. Formulation of the Problem

We use the U.S. Standard Atmosphere [1976] for the ambient neutrals (Figure 1) at altitudes ( $h$ ) of 70 to 100 km with 80% molecular nitrogen ( $N_2$ ), 20% molecular oxygen ( $O_2$ ), and some atomic oxygen (O). Our results are only weakly dependent on the ambient neutral temperature ( $T$ ), taken to

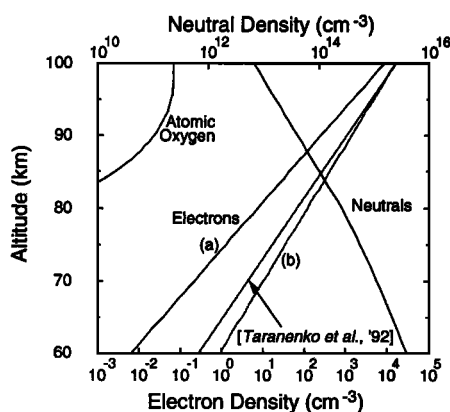


Fig. 1. Ambient profiles of electron and neutral densities. Electron density profile (a) and (b) represent respectively 'tenuous' and 'dense' nighttime D regions. The profile used by Taranenko et al. [1992] is also shown for comparison.

Copyright 1993 by the American Geophysical Union.

 Paper number 93GL02838  
 0094-8534/93/93GL-02838\$03.00

be  $250^\circ \text{ K}$  throughout the region. We consider ambient  $N_e$  profiles representing 'tenuous' (a) and 'dense' (b) nighttime conditions.

We assume the ambient magnetic field to lie in the horizontal plane and the incident EM wave to be planar, with the wave electric field  $\vec{E}$  either i) parallel to  $\vec{B}_0$ , or ii) perpendicular to  $\vec{B}_0$ . Although this configuration is most directly applicable to interactions near the geomagnetic equator, the plasma is collision dominated so that the orientation of  $\vec{B}_0$  plays a minor role in the coupling, as shown in [I].

The description of the EM fields and the dynamics of the electron distribution was given in [I], where it was shown that for the range of altitudes of interest and lightning radiated EM pulses with pulse durations of typically 50-150  $\mu\text{s}$  (e.g., [Uman, 1987], p.112), the current density, ionization, and attachment rates can be approximated by their values derived from the equilibrium solution for a given electric field existing at a particular time, at a given altitude.

For an electric field increasing (decreasing) with time such an approximation leads to an overestimate (underestimate) of the number of high energy electrons due to the fact that the equilibrium is reached from lower (higher) energies. Overall, the error introduced in the calculations of the electron production rate, which is equal to the ionization rate (determined by electrons with energies  $>16 \text{ eV}$ ) minus the dissociative attachment rate (determined by electrons with energies  $>6 \text{ eV}$ ), because of the usage of the quasi-equilibrium solution is  $<10\%$  [I]. Due to a monotonic decrease in the electron distribution function with energy (e.g., Figure 2 (a) of [I]) and the similarity in single peaked dependences of the electron impact excitation cross sections of optical electronic states and dissociative attachment and ionization processes, the error in optical excitation rates would also be  $<10\%$ .

In this paper, we use the same impact excitation model and consider many of the same emission lines as in an earlier paper [Taranenko et al., 1992]. However, instead of assuming a Maxwellian distribution to be maintained and neglecting reflection of the wave, we use the electron distribution function obtained from a self consistent kinetic formulation [I]. The emission lines considered are: the red  $6300 \text{ \AA}$  ( $^1D \rightarrow ^3P$ ), and the green  $5577 \text{ \AA}$  ( $^1S \rightarrow ^1D$ ) lines of O; the blue to UV 2nd positive band ( $C^3\pi_u \rightarrow B^3\pi_g$ ) and red to IR 1st positive band ( $B^3\pi_g \rightarrow A^3\Sigma_u^+$ ) of  $N_2$ ; the blue 1st negative band ( $B^2\Sigma_u^+ \rightarrow X^2\Sigma_g^+$ ) and the IR Meinel band ( $A^2\pi_u \rightarrow X^2\Sigma_g^+$ ) of  $N_2^+$  ions; and the red 1st negative band ( $b^4\Sigma_g^- \rightarrow a^4\pi_u$ ) of  $O_2^+$ . We exclude the  $O_2$  Herzberg I band from our analysis due to lack of reliable electron impact excitation cross sections [T. Slanger, 1992; private communication]. The  $O_2$  atmospheric band is also excluded due to the weak emission intensities in comparison with the backgrounds [Taranenko et al., 1992]. Most electron excitation cross sections are the same as those used in [Taranenko et al., 1992] except that, in accordance with Phelps [1987], the 2nd positive band of  $N_2$  is taken to have a 30% smaller cross section than that proposed by Cartwright et al. [1977] and used in [Taranenko et al., 1992].

## 3. Results

As in [I], we consider the effect on the ionosphere of radiation from a lightning stroke by injecting a  $100 \mu\text{s}$  long EM pulse at the lower boundary (70 km altitude) represented by a

single period oscillation of a sinusoidal wave. We simulate the propagation of the pulse by solving 1-D Maxwell's equations coupled with the Boltzmann equation in the time domain. We run the model for 260  $\mu$ s, which allows the injected pulse to be reflected from the lower ionospheric boundary ( $\sim$ 90 km) and to pass through the interaction region on its way to the ground. We maintain zero field boundary conditions at the upper boundary (120 km) consistent with strong attenuation and reflection in the lower layers. In this paper we present intensities of optical emissions excited as a result of the interaction.

The mean amplitude for cloud-to-ground (CG) flashes as observed at 100 km distance on the ground is  $E_{100} \approx 8.8$  to 11.2 V/m, with amplitudes  $>20$  V/m occurring 3 to 8% of the time [Kridler and Guo, 1983]. Since there is no significant attenuation below 80 km altitude, we refer the injected EM pulse amplitude ( $E_{inj}$ ) to this altitude. Assuming a spherically spreading wave, and leaving aside directional aspects of the radiation from CG versus intracloud discharges [e.g., see Rodriguez et al., 1992], a given  $E_{100}$  corresponds to  $E_{inj} \times \frac{80\text{km}}{100\text{km}}$ . Due to the limitations of the particular numerical model, the largest electric field amplitudes that can be used are  $E_{inj} = 25.5$  V/m (observed  $\sim$ 5% of the time) for profile (a) and  $E_{inj} = 37.5$  V/m (observed  $\sim$ 1% of the time) for profile (b).

3.1 'Tenuous' D Region (Figure 1 (a))

Figure 2 shows snapshots covering the 80 to 180  $\mu$ s time interval in 20  $\mu$ s increments following the injection of the EM pulse with  $E_{inj}=20$  V/m starting at  $t = 0$ . Each frame shows the altitude distribution of the electric field, the average electron energy, and the emission rates of the 'forbidden' 5577  $\text{\AA}$  line of O and the 1st positive 'allowed' band of  $N_2$ . As the wave propagates upward it becomes progressively attenuated and is partially reflected and at 80  $\mu$ s the amplitude at 85 km decreased to  $\sim$ 17.5 V/m. However, due to the partial reflection, the amplitude at 120  $\mu$ s reached 27 V/m at  $\sim$ 83

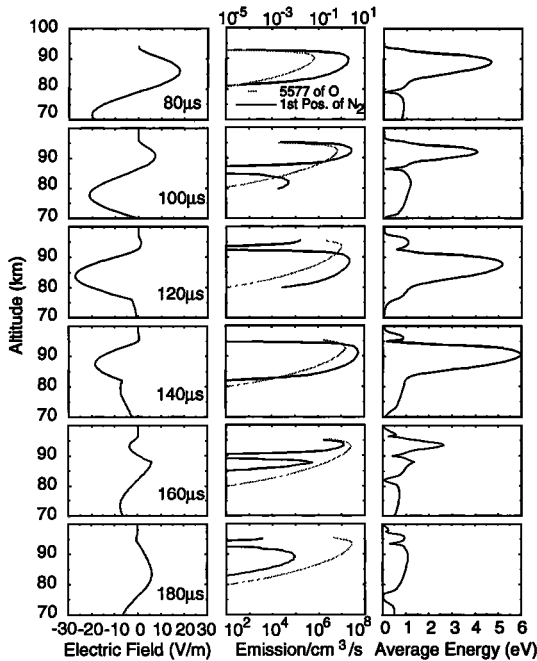


Fig. 2. Snapshots of the electric field, the emission rates for the 1st positive band of  $N_2$  (solid line, lower scale) and the 5577  $\text{\AA}$  line of O (shadow line, upper scale), and average electron energy covering the 80 to 180  $\mu$ s time interval in 20  $\mu$ s increments following the injection of a  $E_{inj} = 20$  V/m EM pulse at 70 km for the case of profile (a) of Fig. 1.

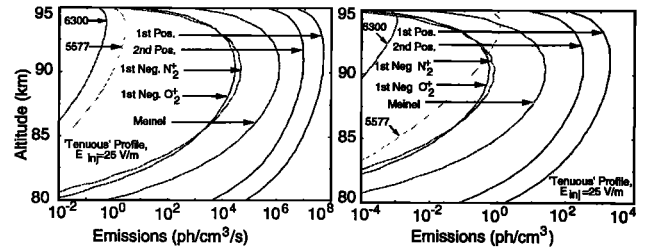


Fig. 3 and 4. (Left) The altitude distributions of maximum intensities stimulated by a  $E_{inj} = 25$  V/m EM pulse for the case of profile (a) of Fig. 1. (Right) The altitude distributions of the emission intensities integrated over the duration of the emissions ( $\sim$ 100  $\mu$ s for the short lasting band emissions,  $\sim$ 0.5 ms at 90 km for the 6300  $\text{\AA}$  line of O, and  $\sim$ 0.1 s at 90 km for the 5577  $\text{\AA}$  line of O) stimulated by a  $E_{inj} = 25$  V/m EM pulse for profile (a) of Fig. 1.

km exceeding the initial amplitude (20 V/m) as a result of constructive interference, as the average energy of the electrons at times exceeds 5 eV, providing a substantial number of electrons with energy higher than the optical thresholds (up to 19 eV). The intensity of the 'forbidden' line (5577  $\text{\AA}$ ) grows throughout the interaction whereas the intensity of the 1st positive 'allowed' band is highly variable and reaches its largest amplitude at the time of constructive interference. The difference in the behaviour of the two emission lines is due to their radiation time intervals,  $\sim$ 0.1 s (due to quenching) at 90 km for 5577  $\text{\AA}$  and  $\sim$ 6  $\mu$ s (time of spontaneous emissions) for the 1st positive.

The altitude distributions of maximum intensities (during the 260  $\mu$ s interaction episode) of the various lines stimulated by a  $E_{inj} = 25$  V/m pulse is shown in Figure 3. The intensities integrated over the duration of the emissions ( $\sim$ 100  $\mu$ s for the short lasting bands,  $\sim$ 0.5 ms at 90 km for 6300  $\text{\AA}$ , and  $\sim$ 0.1 s at 90 km for 5577  $\text{\AA}$ ) are given in Figure 4, whereas the temporal variation of the height-integrated intensities are shown in Figure 5.

Figure 6 shows the maximum emission rates as a function of  $E_{100}$  (i.e.,  $E_{inj} \frac{80\text{km}}{100\text{km}}$ ), with the corresponding percentages of occurrence of discharges with larger  $E_{100}$  separately indicated [Kridler and Guo, 1983].

3.2 'Dense' D Region (Figure 1 (b))

For a 'dense' D region the reflection altitude for the EM pulse is lower, resulting in higher local neutral density and less electron heating.

For the electron density profile (b) in Figure 1 and for an EM pulse with  $E_{inj} = 35$  V/m, the altitude distributions of maximum intensities are shown in Figure 7. The intensities integrated over the duration of the emissions ( $\sim$ 100  $\mu$ s for the short lasting band emissions,  $\sim$ 0.5 ms at 90 km for 6300

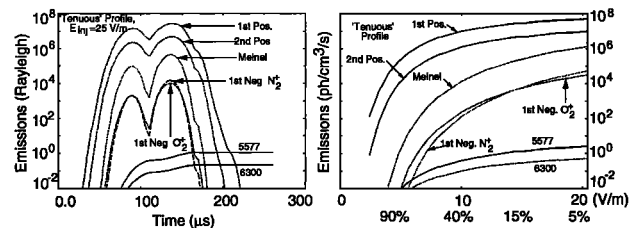


Fig. 5 and 6. (Left) The height integrated intensities (given in Rayleigh's) stimulated by a  $E_{inj} = 25$  V/m EM pulse for profile (a) of Fig. 1. (Right) Maximum emission rates as a function of the electric field amplitude  $E_{100}$  of a pulse for profile (a) of Fig. 1. The percentages of occurrence of discharges with larger  $E_{100}$  are separately given.

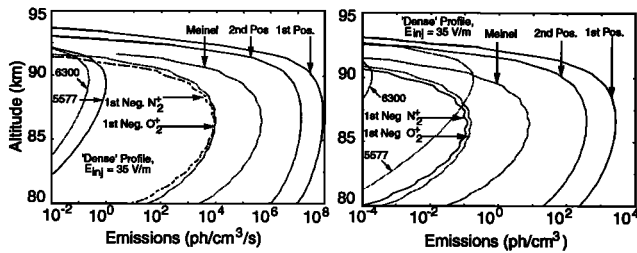


Fig. 7 and 8. (Left) The altitude distributions of maximum intensities stimulated by a  $E_{inj} = 35$  V/m EM pulse for profile (b) of Fig. 1. (Right) The altitude distributions of the emission intensities integrated over the duration of the emissions ( $\sim 100$   $\mu$ s for the short lasting band emissions,  $\sim 0.5$  ms at 90 km for the 6300 Å line of O, and  $\sim 0.1$  s at 90 km for the 5577 Å line of O) stimulated by a  $E_{inj} = 35$  V/m EM pulse for profile (b) of Fig. 1.

Å, and  $\sim 0.1$  s at 90 km for 5577 Å) are given in Figure 9. Comparing these results with the  $E_{inj} = 25$  V/m 'tenuous' case (Figures 3 to 5) we see that significantly larger  $E_{inj}$  are needed to produce comparable optical emission intensities. Figure 10 shows the dependence of maximum emission rates on  $E_{100}$ .

#### 4. Discussion

The generality of our model in terms of accounting for the important aspects of the electrodynamic coupling was discussed in [1]. In the following we compare our results with earlier work and discuss several aspects important for experimental observations.

##### 4.1 Comparison with Taranenko et al. [1992]

Results presented in Figure 3 to 6 of Taranenko et al. [1992] for case A correspond to  $E_{100} = 20$  V/m, i.e., a  $E_{inj} = 25$  V/m pulse. Using the new model for  $E_{inj} = 25$  V/m with the electron density profile used by [Taranenko et al., 1992] indicates that the kinetic calculations give substantially lower intensities compared with the Maxwellian distribution model. Namely, the maximum intensity of the 1st positive band of N₂ is  $5.2 \times 10^7$  cm⁻³ sec⁻¹, i.e., 30 times lower. The corresponding reduction factors for other lines are:  $\sim 90$  for the 2nd positive band of N₂,  $\sim 500$  for the Meinel band of N₂⁺,  $\sim 2700$  for the 1st negative band of N₂⁺,  $\sim 600$  for the 1st negative band of O₂⁺,  $\sim 25$  for 6300 Å, and  $\sim 30$  for 5577 Å lines of O. This result comes about due to several factors. First, due to reflection of the pulse, the maximum heating occurs at  $\sim 88$  km (5 km lower than in the old model). Thus resulting in less heating (6 eV average energy instead of 9 eV). Second, the high energy losses for energies above thresholds of vibrational, optical, dissociative, and ionizational excitations decreases the number of energetic electrons in the tail

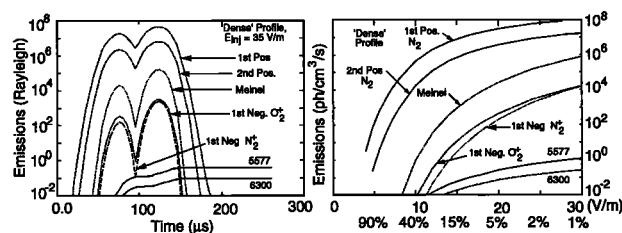


Fig. 9 and 10. (Left) The height integrated intensities (given in Rayleigh's) stimulated by a  $E_{inj} = 35$  V/m EM pulse for profile (b) of Fig. 1. (Right) Maximum emission rates as a function of the electric field amplitude  $E_{100}$  of a pulse for the case of profile (b) of Fig. 1. The percentages of occurrence of discharges with larger  $E_{100}$  are separately indicated.

of the distribution compared with a Maxwellian distribution of the same average energy [1]. For optical emissions with low excitation thresholds the last factor is not as important. For example, for 5577 Å, the 5 km decrease in the altitude of maximum heating results in  $\sim 5.75$  times less electrons and  $\sim 2.75$  times less oxygen atoms, while the decrease in average energy gives a factor of  $\sim 2$  decrease in intensity. Altogether this results in 31.6 times lower emission rate for this line or  $\sim 30$  times as mentioned above. Usage of new cross sections for the 2nd positive band of N₂ does not play an important role in the factor of  $\sim 90$  change.

##### 4.2 Emission Intensities Compared to Airglow

The intensities of the 6300 Å and 5577 Å lines of O have low absolute values for parameters considered here and are more than one order of magnitude below the ambient intensity of the night airglow for zenith observations, which is  $\sim 10^2$  R [Chamberlain, 1978; p. 215].

The intensities of the transitions of N₂ (1st and 2nd positive bands), N₂⁺ (1st negative and Meinel bands), and O₂⁺ (1st negative band) are several orders of magnitude above typical background emission levels in corresponding spectral regions, which are  $\sim 10^3 - 10^4$  R [Chamberlain, 1978; pp. 214-218] for zenith observations.

In terms of detectability with a typical auroral airglow photometer, we note that a good photometer would have a sensitivity of  $\sim 50$  Rayleigh-seconds (R-s) [S. Mende, private communication]. In this context we note that the 1st and 2nd positive bands of N₂ have intensities of 1,200 and 200 R-s and should be detectable from the ground with conventional instruments. However, other emissions have R-s intensities lower than 50 R-s and would have to be observed with specially designed instruments.

##### 4.3 Comparison with Boeck et al. [1992]

We now discuss the reported Space Shuttle observations of transient airglow brightening over a thunderstorm center [Boeck et al., 1992] in the context of our theoretical predictions. Each of the short lasting bands discussed above has transitions with wavelengths from 3600 to 7200 Å to which the TV camera on the Space Shuttle was sensitive with a peak sensitivity at 4400 Å. However, the wavelengths corresponding to the transitions between states with low vibrational numbers of the 1st and 2nd positive bands of N₂, and Meinel band of N₂⁺ are outside the sensitivity range of the camera. Only two strong lines of the 1st negative band of N₂⁺ (0-0 transition at 3914.4 Å and 0-1 transition at 4278.1 Å) lie near the peak of the camera sensitivity. To obtain the intensity of the emissions for limb observations in Rayleighs (i.e., photons/s emitted in a column with 1 cm² cross sectional area along the line of sight multiplied by  $10^{-6}$ ) one must multiply numbers on the abscissa scale of Figure 3 by the thickness of the emitting region in units of 10 km. The  $\sim 50$  μs duration of the emissions implies a  $50 \mu\text{s} \times 3 \times 10^8 \text{ m/s} = 15$  km thickness of the emitting region of simultaneously registered photons at the Shuttle. Multiplying the abscissa of Figure 3 by 1.5 we conclude that the side view intensity averaged over 5 km of altitude of this band is  $\sim 5 \times 10^4$  R. The observed duration of the emissions for the 500 km thickness of the emitting region is  $\sim 1.5$  ms. Hence, the observed effective intensity in R-s at the Space Shuttle would be  $\sim 10$  times lower due to the 1/60 s integration time of the camera, leading to an intensity observed at the Shuttle of  $\sim 5 \times 10^3$  R. Emissions of the 1st negative band of O₂⁺ are in the spectral region of the camera sensitivity ( $\sim 5200-6500$  Å). They have intensity and duration similar to those of the 1st negative band of N₂⁺ and make a comparable contribution to the total effective intensity of  $\sim 10^4$  R of the airglow transient over the visible range. The effective intensity of the emissions is  $\sim 10$  times lower for  $E_{inj} = 20$  V/m than for  $E_{inj} = 25$  V/m.

The intensity of the airglow transient observed from the Shuttle [Boeck *et al.*, 1992] was about twice that of the ambient, which is  $10^3$  R at night [Chamberlain, 1978; pp. 214-218]. Hence, in accordance with the above estimates, only EM pulses with  $E_{inj} \geq 25$  V/m can produce such optical emission intensities. Emissions produced by EM pulses with  $E_{inj} \leq 20$  V/m would not be distinguishable from the background, with the TV camera used in the Boeck *et al.* [1992] experiments.

Since  $E_{inj} = 25$  V/m corresponds to  $E_{100} = 20$  V/m, and such CG discharges occur  $\sim 5\%$  of the time [Krider and Guo, 1983], we conclude that the airglow transient observed by Boeck *et al.* [1992] was due predominantly to emissions of the 1st negative bands of  $N_2^+$  and  $O_2^+$  excited by a relatively intense (and thus relatively rare) lightning discharge.

#### 4.4 Radiative Transfer

Radiative transfer of optical emissions in the atmosphere is important for remote sensing of the heated region, especially for ground based observations.

The 1st and 2nd positive bands of  $N_2$  are not resonantly absorbed in the atmosphere. They originate from transitions between excited levels with a minimum energy of about 6 eV. Hence, resonant absorbers for these emissions practically are not present in the cool ( $\sim 250^\circ$  K) atmosphere. In principle, these emissions could be resonantly absorbed in the heated region; however, the region is optically thin (even in the extreme case of up to  $10^9$  excited particles per cc, with a cross section of  $\sim 10^{-16}$  cm<sup>2</sup>, and a  $10^6$  cm path the optical depth is 0.1). The Meinel and the 1st negative bands of  $N_2^+$  and the 1st negative band of  $O_2^+$  also originate from transitions between excited levels with minimum energy of  $\sim 15$  eV so that the same arguments above also apply to them.

Rayleigh scattering is the major factor that determines the optical thickness of the clear atmosphere for the bands and which results in reduction in intensity of up to 4 % for red and up to 25 % for blue spectral ranges per vertical traverse through the atmosphere [Fenn *et al.*, 1985]. Namely, the 1st positive band of  $N_2$  and the 1st negative band of  $N_2^+$  have blue to near UV lines and are subject to  $\sim 25$  % reduction of their intensity for ground based observations, whereas the 1st positive band of  $N_2$ , the Meinel and the 1st negative bands of  $N_2^+$  emit in red and IR parts of the spectrum range and are reduced by  $< 4$  % for ground based observations. For observations from a high altitude ( $\sim 20$  km) aircraft Rayleigh scattering loss decreases to a few percent for any of the bands.

#### 5. Summary

Our results indicate that EM radiation originating in lightning discharges excites optical emissions with substantial intensities in the nighttime lower ionosphere. The most promising for observations are the 1st and 2nd positive bands of  $N_2$ , the emission rates for which reach  $7 \times 10^7$  and  $10^7$  cm<sup>-3</sup> s<sup>-1</sup> respectively at an altitude of  $\sim 92$  km for a  $E_{inj} = 25$  V/m EM pulse for the 'tenuous' D region. The maximum height integrated intensities of these emissions are  $4 \times 10^7$  and  $6 \times 10^6$  R. The 1st negative band of  $N_2^+$  has maximum emission rate of  $5 \times 10^4$  cm<sup>-3</sup> s<sup>-1</sup> at  $\sim 90$  km and the maximum height integrated intensity of  $10^4$  R. The Meinel band of  $N_2^+$  has the maximum emission rate of  $\sim 10^6$  cm<sup>-3</sup> s<sup>-1</sup> at  $\sim 90$  km and the maximum height integrated intensity of  $6 \times 10^5$  R. The 1st negative band of  $O_2^+$  has the maximum emission rate of  $3 \times 10^4$  cm<sup>-3</sup> s<sup>-1</sup> at  $\sim 90$  km and the maximum height integrated intensity of  $10^4$  R. All of these emissions last for  $\sim 50$   $\mu$ s and have intense lines in the window of atmospheric transparency and are expected to be above the nighttime backgrounds for short exposure times ( $\sim 1$  ms) for space-borne, ground-based,

or aircraft-based observations. The 6300 and 5577 Å lines of O have intensities that are several times below the background at night and are not convenient for observations. The current kinetic model gives 30 to 2,700 times lower emission rates for the same electric field in comparison to one which assumed a Maxwellian distribution and neglected reflections from the ionosphere [Taranenko *et al.*, 1992]. The Space Shuttle observations of transient airglow brightening [Boeck *et al.*, 1992] are interpreted as emissions of the 1st negative bands of  $N_2^+$  and  $O_2^+$  in the tenuous D region stimulated by a strong lightning discharge with  $E_{100} > 20$  V/m.

**Acknowledgments.** This work was supported by NASA under contract NAGW-2871. We thank our colleagues in the STAR Laboratory and Dr. T. Slanger of SRI International for useful discussions and the referees, for their constructive criticisms.

#### References

- Allis, W.P., Motions of ions and electrons, *Encyclopedia of Physics*, vol. 21, p. 404, Berlin: Springer-Verlag, 1956.
- Boeck, W.L., O.H. Vaughan, Jr., R. Blakeslee, B. Vonnegut, and M. Brook, Lightning induced brightening in the airglow layer, *Geophys. Res. Lett.*, vol. 19, pp. 99-102, 1992.
- Cartwright, D.C., S. Trajmar, A. Chutjian, and W. Williams, Electron impact excitation of the electronic states of  $N_2$ . II. Integral cross sections at incident energies from 10 to 50 eV, *Phys. Rev. A*, vol. 16, pp. 1041-51, 1977.
- Chamberlain, J.W., *Theory of planetary atmospheres*, Academic Press, New York, 1978.
- Fenn, R.W., S.A. Clough, W.O. Gallery, R.E. Good, F.X. Kneizys, J.D. Mill, L.S. Rothman, E.P. Shettle, and F.E. Volz, Optical and infrared properties of the atmosphere, in *Handbook of Geophysics and the Space Environment*, p. 18-1 to 18-80, AFGL, Hancolm, MA, NTIS, 1985.
- Inan, U.S., D.C. Shafer, W.Y. Yip, and R.E. Orville, Subionospheric VLF signatures of nighttime D-region perturbations in the vicinity of lightning discharges, *J. Geophys. Res.*, vol. 93, p.11,455, 1988.
- Inan, U.S., T.F. Bell, and J.V. Rodriguez, Heating and ionization of the lower ionosphere by lightning, *Geophys. Res. Lett.*, vol. 18, pp. 705-708, 1991.
- Krider, E.P., and C. Guo, The peak electromagnetic power radiated by lightning return strokes, *J. Geophys. Res.*, vol. 88, p. 8471, 1983.
- Phelps, A.V., Excitation and ionization coefficients, *Gaseous Dielectric*, vol. 5, 1987, p. 1-9, 1987.
- Rodriguez, J.V., U.S. Inan, and T.F. Bell, D region disturbances caused by electromagnetic pulses from lightning, *Geophys. Res. Lett.*, vol.19, pp. 2067-2070, 1992.
- Taranenko, Y.N., U.S. Inan, and T.F. Bell, Optical signatures of lightning-induced heating of the D region, *Geophys. Res. Lett.*, vol. 19, pp. 1815-1818, 1992.
- Taranenko, Y.N., U.S. Inan, and T.F. Bell, Interaction with the lower ionosphere of electromagnetic pulses from lightning: heating, attachment, and ionization, *Geophys. Res. Lett.*, vol. 20, pp. 1539-1542, 1993.
- Uman, M.A., *The lightning discharge*, Academic Press, Orlando, 1987.
- U.S. Standard Atmosphere, 1976*, NOAA-S/T 76-1562, U.S. Government Printing Office, Washington, D.C., 1976.

Y. N. Taranenko, U. S. Inan, and T. F. Bell, Space, Telecommunications And Radioscience Laboratory, Department of Electrical Engineering/SEL, Stanford University, Stanford, CA 94305.

(Received June 24, 1993;  
revised September 2, 1993;  
accepted September 22, 1993.)